Simulation of NH3 Temperature-Programmed Desorption Curves Using an ab Initio Force Field

ARTICLE *in* THE JOURNAL OF PHYSICAL CHEMISTRY C · SEPTEMBER 2009

Impact Factor: 4.77 · DOI: 10.1021/jp811413m

3 AUTHORS, INCLUDING:

Lifeng Zhao
National Institute of Biological Sciences, C…

12 PUBLICATIONS **92** CITATIONS

SEE PROFILE

Simulation of NH_3 Temperature-Programmed Desorption Curves Using an ab Initio Force Field

Lianchi Liu, Lifeng Zhao, and Huai Sun*

School of Chemistry and Chemical Engineering, Shanghai Jiao Tong University, Shanghai 200240, China

Received: December 25, 2008; Revised Manuscript Received: June 30, 2009

Temperature-programmed desorption curves for ammonia (NH_3-TPD) were predicted successfully using grand canonical ensemble Monte Carlo simulation methods and force field parameters derived from quantum mechanical ab initio data. This approach provides a means to study the relationship between the structure and acidity of zeolites at the molecular level. Analysis of the predicted NH_3-TPD curves reveals that zeolite pore size is a critical factor influencing the curve shape. The so-called weak and strong acids of zeolites, which give rise to two peaks in the TPD curve, are roughly related to the interactions among ammonia molecules in the pores and to the interactions between ammonia molecules and the zeolite pore walls, respectively. However, the NH_3-TPD curves may still show a double peak feature without any strong acid centers if the pore is such a size that additional strain is put on the NH_3 hydrogen-bond network.

1. Introduction

The acidity of a zeolite is directly linked with its catalytic efficiency and thus is one of the most critical factors to consider when designing new zeolite materials.[1−5] For example, it has been reported that especially strong acidity can be achieved by growing beta zeolite (BEA) and mordenite (MOR) together.[6] The resulting material shows higher acidity in comparison with a mechanical mixture of the two zeolites. One proposed explanation for the excess acidity is that the interphase between the different zeolites has an abnormally high concentration of Brønsted acid centers. However, this hypothesis is difficult to prove experimentally. A reliable method for predicting acidity based on the microscopic structure of zeolites is needed to address problems like this.

Various experimental techniques have been developed to study the nature, concentration, strength, and distribution of the acid sites in zeolites.[7−9] Most of these methods are based on the adsorption of probe molecules. Conventional methods, such as temperature-programmed desorption using ammonia molecules (NH_3-TPD) and adsorption calorimetry of adsorbed probe molecules, provide information regarding the strengths and distribution of the active sites. Spectroscopic methods, such as infrared and NMR spectroscopy, have been used to study the structures of the acid sites. All these methods, however, involve complicating factors, such as diffusion of the molecules, zeolite defects, and impurities. Interpreting the data to determine zeolite acidity, therefore, continues to be the subject of a discussion which is far from being settled.[10−13]

To avoid the difficulties of the experimental methods, researchers have used computational approaches to probe the acidity of zeolites. Quantum chemistry methods at the Hartree−Fock (HF) and the second order Møller−Plesset perturbation theory (MP2) levels of theory, for example, have been used to study the strength of interactions between the small probe molecules (NH_3) and the Brønsted acid sites using cluster models.[10−12] Teunissen et al.[11] introduced the long-range electrostatic interactions and boundary condition into cluster models for calculating the NH_3−zeolite interactions. Bolis et al.[12] compared experimental data of microcalorimetry and IR spectroscopy with ab initio calculation results. Sauer et al. did a series of work[13−16] on the acidity of Brønsted acids of zeolites using hybrid quantum mechanics and molecular mechanics (QM/MM) methods. Molecular simulations have been carried out to study the molecular adsorption and diffusion in zeolites by many investigators. Among them, Henninger and Nunez studied the adsorption of ammonium ion in the H-ZSM zeolites[17] using the augmented consistent valence force field. Teraishi and Akanuma studied the adsorption of ammonia and pyridine in MFI[18] based on a Burchart force field. Jaramillo[19] calculated the adsorption of NH_3, CO_2, and H_2O in the LTA (Linda type A) zeolites. Surprisingly, despite the fundamental importance of NH_3-TPD curves on zeolites, such curves have not previously been predicted using molecular simulation methods.

Because NH_3-TPD is, perhaps, the most commonly used technique for studying the acidity of zeolites, a direct comparison of simulated and experimental adsorption curves would be useful for understanding the nature, distribution, and strengths of the acid centers in zeolites. The lack of a high-quality force field is likely a key reason that NH_3-TPD curves have not yet been predicted through computation. Most force fields proposed in the literature[20−24] are designed for modeling the bulk properties of zeolites, in which the nonbond interactions between the framework and guest molecules are not well represented.

In this work, we applied quantum chemistry calculations to characterize the potential energy surfaces between the ammonium molecule and the zeolite framework with and without a Brønsted acid center. On the basis of ab initio data, we developed a force field and predicted the NH_3-TPD curves using grand canonical ensemble Monte Carlo (GCMC) simulations. The simulations were performed with different pore sizes, Si/Al ratios, and acid site locations. By comparing the calculated data with experimental data, we attempt to shed light on the origin of zeolite acidity and to establish a computational approach to measure the acidity of zeolites with different geometric and chemical structures.

* Corresponding author. Phone: +86-21-5474-8987-601. Fax: +86-21-5474-1297. E-mail: huaisun@sjtu.edu.cn..

10.1021/jp811413m CCC: $40.75
Published on Web 08/17/2009

2. Models and Methods

The force field parameters were derived from ab initio energy data calculated for clusters of the ammonia molecule and zeolite model compounds. Two molecules representing the zeolite structures were constructed (Figure 1). One of the model molecules, (A), is a pure silica molecule containing five tetrahedral silicon atoms and another, (B), is a molecule with the Brønsted acid center built from the pure silica model by replacing the central Si with Al and adding a bridge hydrogen. The initial structures of zeolite model molecules were taken from the straight channel in MFI zeolite and optimized at the B3LYP/SV(P) level of theory with the dangling bonds saturated with hydrogen atoms and fixed. The interaction energies between the ammonia and zeolite model molecules were calculated at the RI-MP2/TZVPP level of theory. In these calculations, the model molecules representing zeolite were fixed at the structures obtained at the B3LYP/SV(P) level, and the NH_3 molecule was fully relaxed. The binding energy was calculated as

$$\Delta E = E_{NH_3-model} - E_{model} - E_{NH_3} \quad (1)$$

where the $E_{NH_3\text{-model}}$ is the total energy of the cluster, E_{model} is the energy of the zeolite model molecule, and E_{NH_3} is the energy of ammonia. As ammonia approaches the Brønsted acid site, the proton is transferred from the acidic center to ammonia. In this case, the binding energy between the protonized ammonium ion and the deprotonized Brønsted acid site was calculated as the total energy of the cluster ($E_{NH_3\text{-model}}$ in eq 1). The basis set superposition error (BSSE) was subtracted in the interaction energies.[25] The ab initio calculations were carried out with the TURBOMOLE 5.8 software package.[26]

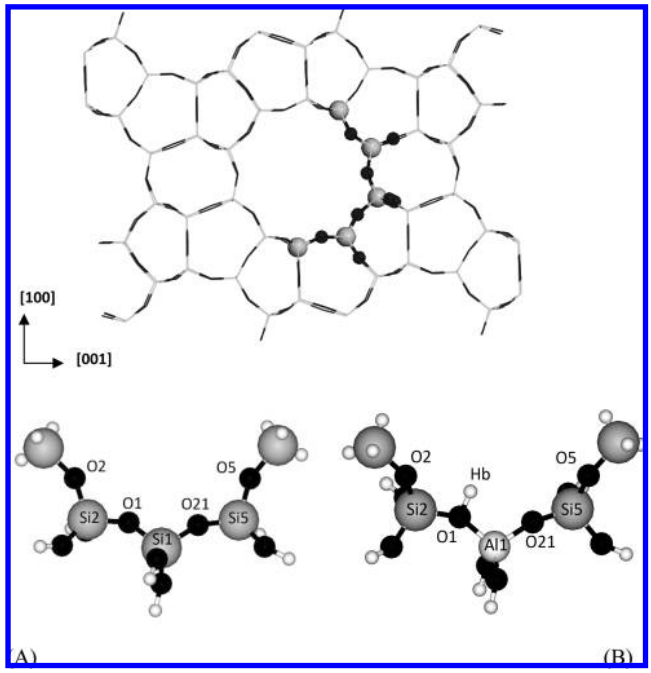

Figure 1. Zeolite model molecules. The silica model (A) and acidic model (B) are used for the ab initio calculations. The small white ball represents H, the black ball represents O, the small gray ball represents N, the big gray ball represents Si, and the big white ball represents Al. The model structure was taken from the straight channel of the MFI zeolite.

In the simulations, the zeolites were treated as rigid bodies and their atomic coordinates were taken from experimental data. The Lennard−Jones (LJ) 12-6 and Coulombic terms were used to describe the interactions between the ammonia molecule and zeolites:

$$E = E_{LJ12-6} + E_{coul} = \sum_{i<j} \left\{ \varepsilon_0 \left[\left(\frac{\sigma_0}{r_{ij}} \right)^{12} - 2 \left(\frac{\sigma_0}{r_{ij}} \right)^{6} \right] + \frac{q_i \cdot q_j}{r_{ij}} \right\} \quad (2)$$

The Lorentz−Berthelot mixing rule was used for LJ interactions between unlike atoms:

$$r_{ij} = (r_i + r_j)/2 \qquad \varepsilon_{ij} = \sqrt{\varepsilon_i \varepsilon_j} \quad (3)$$

The charge model proposed by Kramer et al.[41] was used for zeolites; the OPLS force field[27] was applied for the NH_3 molecule. These models have been used successfully for neat zeolites or NH_3; therefore, we did not modify those parameters. We only adjusted the newly introduced nonbond parameters describing the interactions between the NH_3 and zeolites. Since classical force fields and simulation software do not allow bond dissociations, we applied the NH_3 model in computations of the entire potential energy surface. The energy differences between the ammonia (NH_3) and protonized ammonium ion (NH_4^+) models near the Brønsted acid site were evaluated based on RI-MP2 calculations.

The GCMC method[28−30] was used to simulate the adsorption of NH_3 in zeolites. The Monte Carlo moves were divided into insertion, deletion, translation, rotation, and vibration with probabilities of 30%, 30%, 10%, 15%, and 15%, respectively. The van der Waals (VDW) interactions were calculated using a cutoff value of 12 Å and compensated with the tail corrections; the electrostatic interactions were calculated using the Ewald summation method. The simulations were performed in the temperature range from 300 to 900 K at intervals of 50 K. At each temperature, 10^6 moves were carried out for equilibration and 10^6 moves for data collection. The chemical potentials required for the GCMC simulations were calculated using the Widom insertion method[31] performed on gaseous NH_3 at the same thermodynamic conditions. The Monte Carlo simulations were performed with the TOWHEE software package.[32]

Molecular dynamics (MD) simulations were performed with the predicted uploads of ammonia to analyze the energies and structures of absorbed molecules in the zeolites. A time step of 1 fs was used, and the simulations were performed for 500 ps for equilibration and at 1 ns for data collection. The nonbond interactions were treated in the same fashion as that used in the MC simulations. The electrostatic interactions were evaluated using the particle mesh Ewald method. The GROMACS package was used for the MD simulation.[33]

Three zeolites were investigated: an 8-membered ring (8-MR) ACO, a 10-membered ring (10-MR) MFI, and a 12-membered ring (12-MR) MOR. The atomic coordinates and cell parameters were taken from experimental data.[34−36] Supercells of 2 × 2 × 2 were built for the simulations. Si/Al ratios of ∞, 95, and 11 for MFI and ∞, 15, and 11 for MOR were considered. The positions of the added aluminum atoms were randomly chosen.

3. Results and Discussion

3.1. Ab Initio Calculations. Figure 2 shows the optimized structures of the clusters of ammonia and zeolite model molecules at the RI-MP2/TZVPP level of theory. With the pure

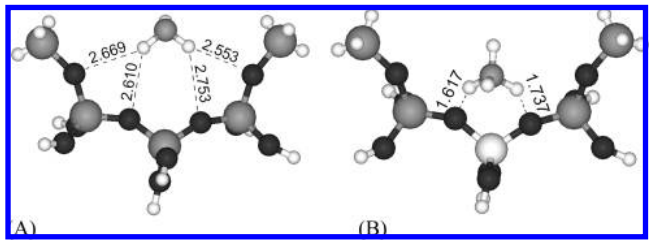

Figure 2. Structures of (A) ammonia with the pure silica zeolite model and (B) ammonia with the acidic zeolite model optimized at the RI-MP2/TZVPP level of theory. The atoms are represented using the same color balls as given in Figure 1. The hydrogen bond lengths (in Å) are labeled.

silica model (Figure 2A), two of the three hydrogen atoms of ammonia form hydrogen bonds with four oxygen atoms in the zeolite model. The average distance of the hydrogen bonds is about 2.65 Å. With the acidic model (the zeolite with Al atom), the optimized structure (Figure 2B) indicates that the proton is transferred from the zeolite to ammonia, forming an ammonium ion (NH_4^+). The interaction between the ammonia and zeolite, therefore, is ionic in nature. The nitrogen is much closer to the zeolite in the acidic model than in the pure silica case, and two of the four hydrogen atoms in the ammonium ion interact with two oxygen atoms of the zeolite. The average distance between the hydrogen and oxygen atoms is only about 1.68 Å. These results are consistent with those reported in the literature.[1,2]

We investigated the proton transfer using a small zeolite model compound, SiH_3OHAlH_3, interacting with an ammonia molecule with the lone-pair orbital pointing toward the Brønsted acid hydrogen, as shown in Figure 3. In these calculations, the nitrogen−oxygen distance was varied from 2.35 to 2.6 Å at 0.01 Å intervals, and the O−H distance was varied from 1.0 to 1.5 Å at 0.02 Å intervals. At each point, the energy was calculated at the RI-MP2/TZVPP level of theory. The contour map of the scanned energies is illustrated in Figure 3. From the energy map it is clear that there is no energy barrier for the proton transfer. The minimum energy is located at the cross point of 2.5 Å of the N−O bond and 1.3 Å of the O−H bond (corresponding to 1.2 Å of the N−H bond). This result reveals that the minimum energy corresponds to a structure where the proton stays between the ammonia and the zeolite. It also indicates that the potential surface is quite flat and the proton

TABLE 1: Binding Energies of Ammonia with Zeolite Model Molecules (see Figure 2)

model A (kcal/mol)	model B (kcal/mol)
1.02	20.18
	20.06[a]

[a] Wthout proton transfer.

easily oscillates between the oxygen and nitrogen atoms. In the minimized structure of the larger model, as shown in Figure 2B, the proton is transferred to the nitrogen due to additional forces from adjacent atoms in the zeolite model.

Table 1 lists the calculated binding energies of the ammonia−zeolite clusters. The binding energy computed in this work is −1.02 kcal/mol for the pure silica model and −20.18 kcal/mol for the acidic model. The remarkable difference in binding energies between these two models highlights the importance of the acid site for zeolite activity. The actual position of the proton does not matter greatly. We calculated the binding energy of ammonia without proton transfer (the NH_3 model) by fixing the H−O bond length, and the result obtained is −20.06 kcal/mol, extremely close to that obtained using the proton transfer (the NH_4^+) model. Therefore, we were confident to use the NH_3 model to explore the potential energy surfaces.

3.2. Force Field. To develop the force field parameters describing the nonbond interaction between ammonia and zeolite, a total of 160 configurations of the ammonia and zeolite model molecules were generated. Both the pure silica and the acidic zeolite model molecules were considered, and the ammonia molecules were positioned randomly in the vicinity of the central region of the zeolite model compounds. The binding energy for each of these generated configurations was calculated at the RI-MP2/TZVPP level of theory.

The LJ and charge parameters for ammonia were taken from the OPLS force field. The charges of atoms in the zeolite were taken from the literature[41] as +2.4 for Si, −1.2 for O, +2.0 for Al, and +0.4 for H. The interaction between the ammonia and zeolites was determined by adjusting the LJ parameters of Si, O, Al, and H atoms in the zeolite to fit the ab initio data calculated. The fit was generally satisfactory, and a comparison of the binding energies computed using the force field and the MP2 method is presented in Figure 4. Because of the simplicity of the functional forms and limited number of adjustable

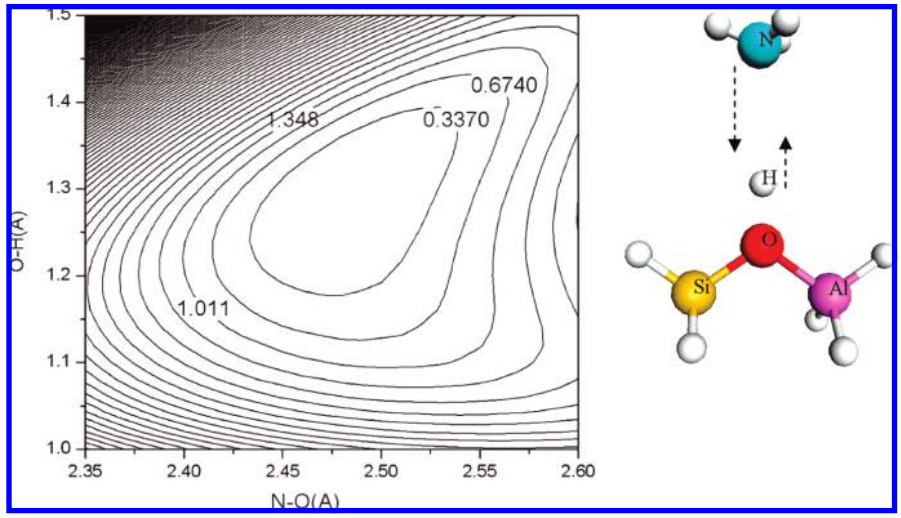

Figure 3. Proton transfer energy surface between ammonia and the Brønsted acid model. The contour lines represent the relative energy with the lowest energy as the base energy. The unit is kcal/mol.

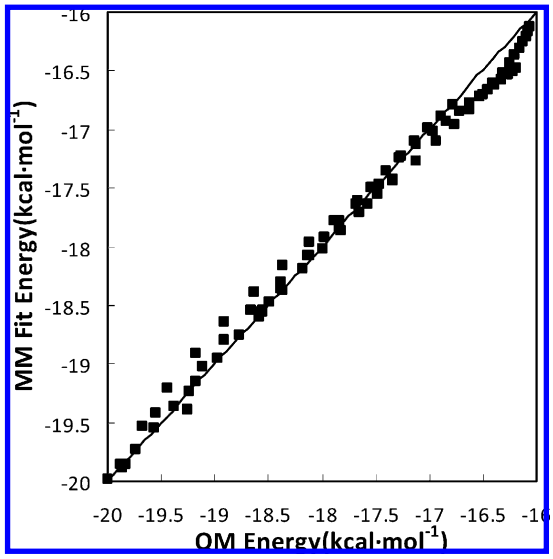

Figure 4. Comparison of energies computed using the RI-MP2/TZVPP (QM) and force field (MM) methods.

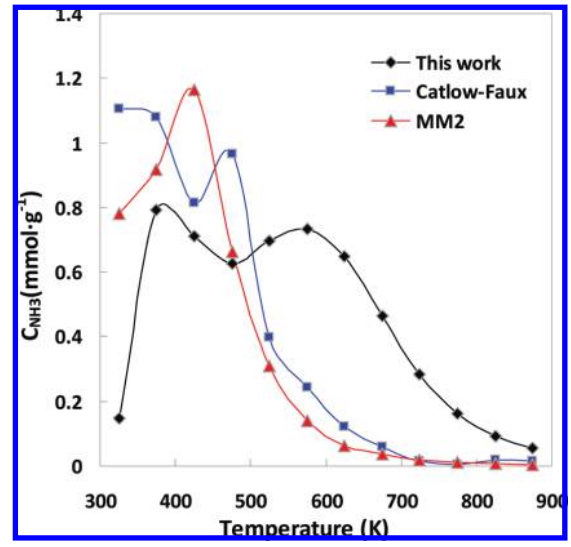

Figure 5. NH_3-TPD curves calculated using different force fields for the pure MFI zeolite.

TABLE 2: Optimized Nonbond Parameters

	σ (Å)	ε (kcal/mol)	q
Si	3.914	0.2638	+2.4
O	2.760	0.4267	−1.2
Al	3.936	0.0193	+2.0
Hb			+0.4

TABLE 3: Comparison of Calculated and Experimental Adsorption Energies of Ammonia in Different Zeolites (kcal/mol)

zeolite	this work		QM/MM[13]		experiment	
	Si/Al	ΔE	Si/Al	ΔE	Si/Al	ΔE
HZSM-5	31	26.42	95	26.05	25−33[8]	24.9−26.3
					>27[37−39]	34.7−35.9
					20−70[40]	31.3−31.8
HMOR	31	28.87	47	28.44	12−39[43]	27.49−27.96
ACO	15	22.69				

parameters, only the bottom section of the potential energy surfaces could be well-represented. As shown in Figure 4, a discrepancy above ca. −17 kcal/mol is noticeable.

The NH_3 binding energies obtained using the force field are −1.0 kcal/mol for the pure silicate model (A) and −20.1 kcal/mol for the acidic model (B). The optimized nonbond parameters of zeolite are listed in Table 2. The LJ parameters are similar to those derived for organic molecules (such as in OPLS) except the σ of oxygen is clearly smaller than a normal value. The LJ parameters for the hydrogen atom are zero, as they are for the SPC[42] and other water models.

To validate the force field parameters, we calculated the adsorption energies of NH_3 in various zeolites. The calculations were performed on zeolite lattices using the periodic boundary conditions and long-range interaction corrections, as explained in section 2, above. Table 3 lists the computed data together with QM/MM[13] and experimental[8,37−40,43] results for comparisons. Our data and the QM/MM data agree well with two sets of the experimental data[8,43] for HZSM-5 and HMOR, zeolites respectively. However, other experimental adsorption energies[37−40] are significantly higher. As discussed by previous investigators,[13] the Si/Al ratios, defects and impurities in the measured samples, and the measurement methods may contribute significantly to the results. It is encouraging that our data agree with the QM/MM[13] and experimental data[8,43] not only on the absolute but also on the relative values among different zeolites. We did not find any calculated or experimental data for direct comparison for ACO zeolite. Among the three zeolites calculated, the adsorption energy of NH_3 in ACO is the lowest.

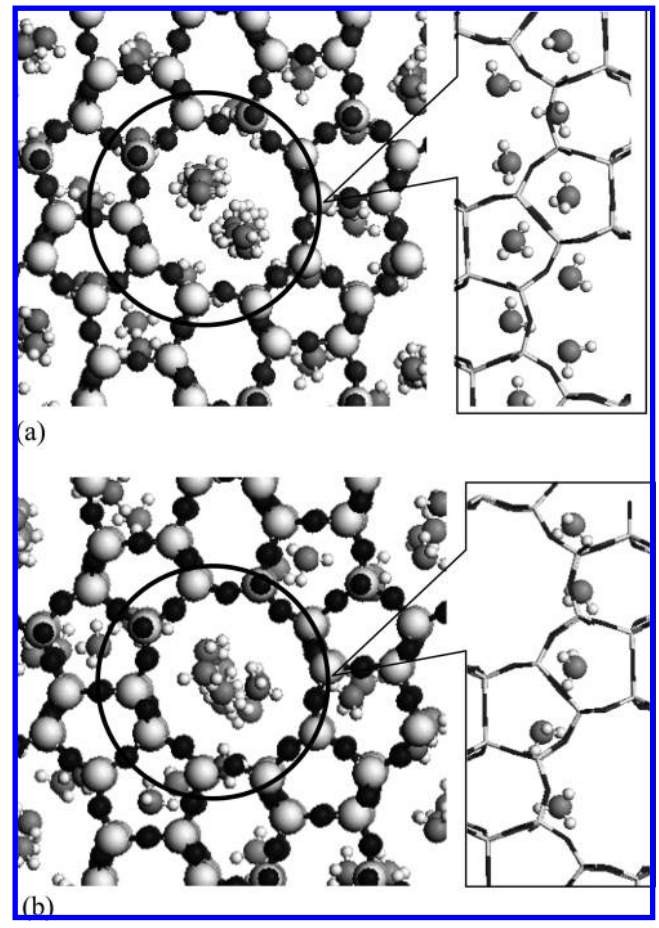

Figure 6. Snapshots of ammonia molecules in the pure silica MFI zeolites at (a) 300 K and (b) 450 K. The ammonia molecules in the straight channel are viewed from the side.

3.3. Prediction of NH_3-TPD Curves in Pure Silica Zeolites. The simulated NH_3-TPD curves in pure MFI zeolite using our force field and two force fields reported in the literature are

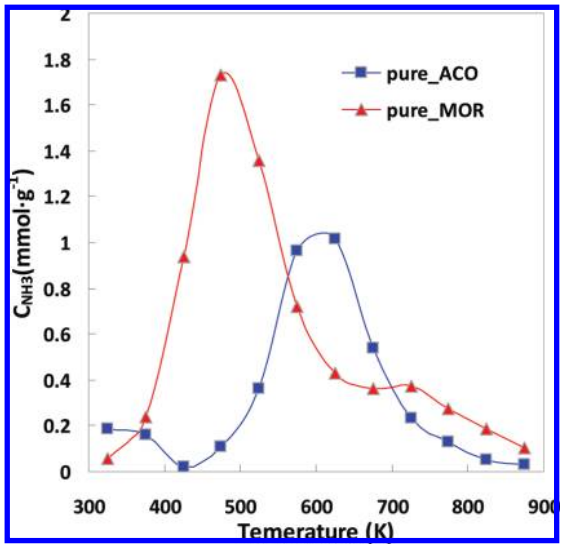

Figure 7. NH_3-TPD curves calculated for 8-MR ACO and 12-MR MOR.

presented in Figure 5. With the ionic Catlow−Faux[3] force field, two peaks are predicted, but the peak temperatures are too low; the ammonia molecules are desorbed too early from the zeolite. With the MM2[4] force field, the predicted NH_3-TPD curve has only one peak at ca. 430 K. With the newly developed force field, we obtained a two-peak curve in which the low-temperature peak is at about 380 K and the high-temperature peak is at about 580 K.

We have not found any NH_3-TPD curves of pure-silica zeolites in the literature for a direct comparison. We, therefore, consider the NH_3-TPD curves measured for almost pure silica HMFI zeolite with a Si/Al ratio of 120, in which two peaks are observed at 460 and 690 K.[5] Our calculated curve is consistent with this experimental data, although the peak temperatures are lower by about 100 K. This underestimate is understandable due to the differences between the computational model and the real experimental sample.

The first and second TPD peaks are commonly referred to as weak and strong acid sites. To investigate what the two peaks correspond to at the molecular scale for the nonacidic zeolite, we have taken snapshots from the TPD simulation. Two snapshots of ammonia molecules adsorbed in the pure MFI zeolites before and after the first peak (at 300 and 450 K) are displayed in Figure 6. These images indicate that the desorption of ammonia is divided into two stages. At low temperature, the ammonia molecules are packed in the straight channel of MFI and lined up in roughly two rows, and they interact with each other through hydrogen bonds. As the temperature increases, the hydrogen bond network is reorganized, and by 450 K, the distribution of ammonia molecules in the channel has changed significantly. The ammonia molecules are now in only one row. The hydrogen bond network is apparently more stable at the higher temperature due to more free space in the pore that allows the ammonia molecules to rotate into orientations that allow stronger hydrogen bonds.

The NH_3-TPD curves were also calculated for nonacidic MFI zeolites with different pore sizes. Figure 7 presents the simulation results of the 8-MR ACO and 12-MR MOR zeolites. In contrast to the 10-MR MFI, as discussed above, both the ACO and the MOR show only one peak in the simulated NH_3-TPD curves. Figure 8 shows snapshots of the projected distributions of ammonia molecules in the ACO and MOR models at different temperatures. Note that the ammonia molecules are in pore channels either perpendicular to the paper plane or parallel to the paper plane, as noted in Figure 8. In ACO, shown in Figure 8a, the ammonia molecules are lined up in one row in the perpendicular pore channel. In MOR, shown in Figure 8b, they form roughly four rows in the large (12-MR) perpendicular pore channel. As the temperature increases, the ammonia molecules gradually desorb from the ACO channels by breaking their intermolecular hydrogen bonds. In MOR, the ammonia configurations are more complex,

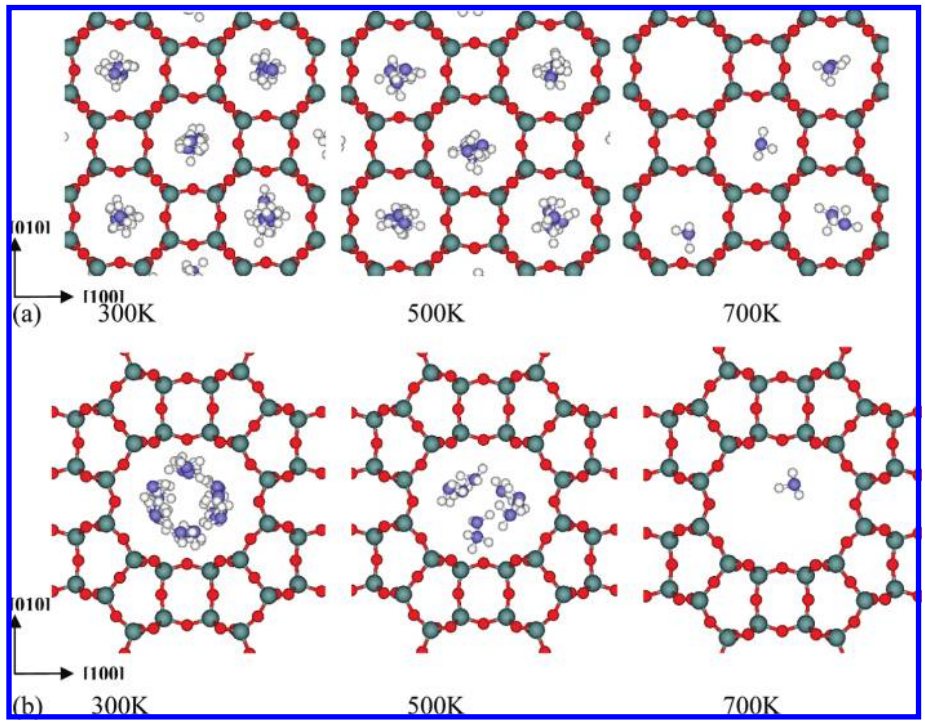

Figure 8. Snapshots of the projected distribution of ammonia molecules in (a) 8-MR ACO and (b) 12-MR MOR at different temperatures. The molecules in pores parallel to the paper plane are omitted for clarity.

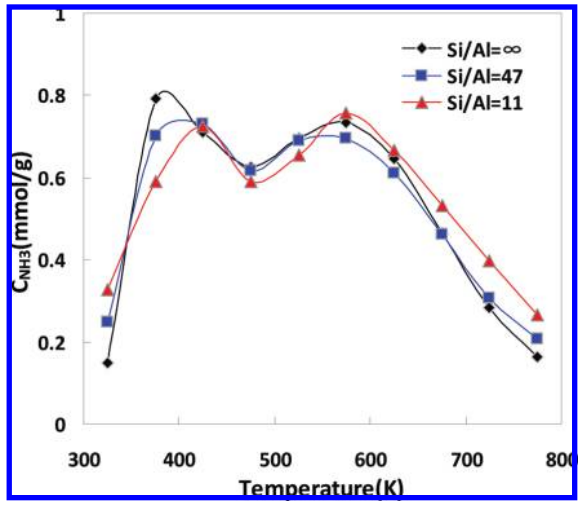

Figure 9. Concentration of ammonia versus temperature, representing the desorption of ammonia from MFI zeolites with different Si/Al ratios. (◆), (■), and (▲) correspond to Si/Al ratios of ∞, 47, and 11, respectively.

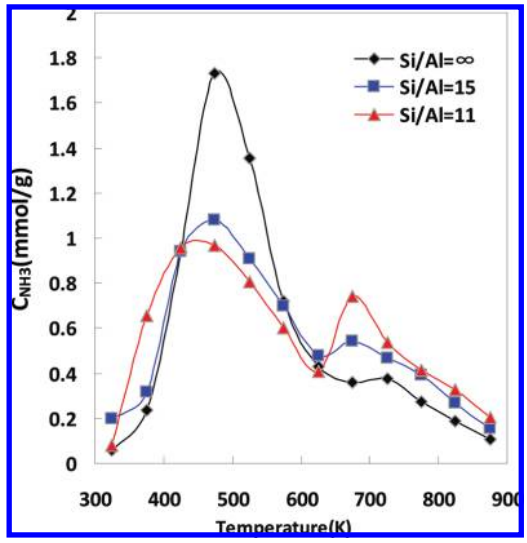

Figure 10. Desorption of ammonia from MOR zeolites with different Si/Al ratios. (◆), (■), and (▲) correspond to a Si/Al ratio of ∞, 15, and 11, respectively.

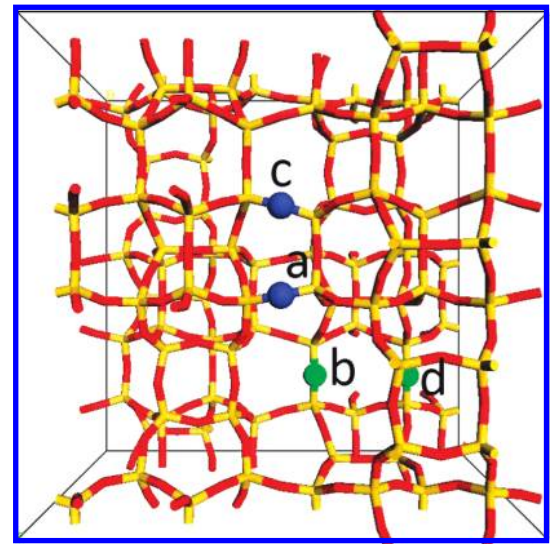

Figure 11. Four different acid sites in an MFI zeolite. Sites *c* and *d* are in the straight channel, and *a* and *b* are in the zeta channel.

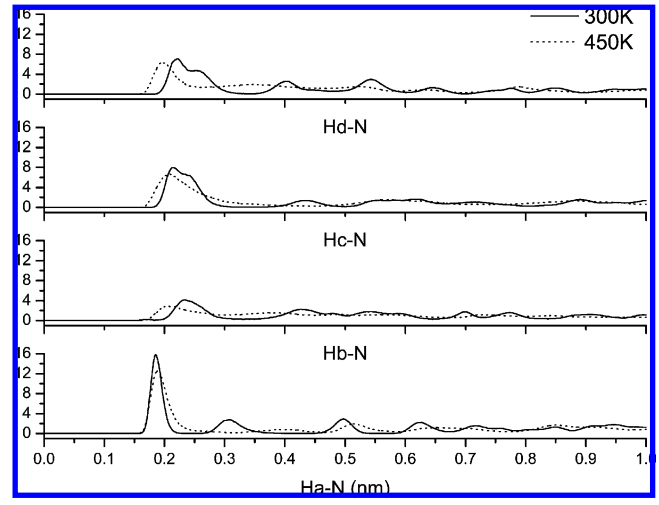

Figure 12. Radial distribution functions of acidic hydrogen and ammonia nitrogen atom pairs calculated for the four different acid sites, *a*, *b*, *c*, and *d*, at 300 K (solid lines) and 450 K (dashed lines).

as shown in Figure 8b. As the temperature increases, the number of molecules in the pores decreases. Because the large 12-MR pore provides enough free space for the adsorbed molecules, the remaining molecules do not gain significant additional stability. Therefore, only one desorption peak presents in the NH_3-TPD curve. The predicted desorption temperatures are consistent with the mechanisms discussed above. The peak desorption temperature for ACO is 460 K, which is between the two peaks of MFI. The peak temperature for MOR is 600 K, a little higher than the second peak of MFI. It should be noted that the peak shape and position for MOR agree well with experimental measurement.[43] To our knowledge, experimental results have not been reported for ACO.

3.4. TPD Prediction for Zeolites with Different Si/Al Ratios. Figures 9 and 10 present the simulated NH_3-TPD curves for MFI and MOR zeolites with different Si/Al ratios. In Figure 9, the curves for MFI with Si/Al ratios of ∞, 47, and 11 show that the low-temperature peak becomes weaker and the high-temperature peak becomes stronger as the Si/Al ratio decreases. This is consistent with experimental measurements.[5] As the acidity increases with Al, the ammonia molecules stay longer in the zeolite due to stronger binding. Figure 10 shows how increasing acidity changes the NH_3-TPD curve in MOR. Although there is only one peak in pure MOR, as the Si/Al ratio decreases, another peak at higher temperature (680 K) emerges and becomes stronger with increasing acidity. The same phenomenon has been observed in experiments, and the peak temperatures also agree well with the experimental ones.[6]

In the literature, double peaks are commonly referred to as weak and strong acid centers. Our analysis shows that both peaks are controlled jointly by the size of the pore and the position and number of acidic centers. Roughly speaking, the weak acidity is primarily related to interactions among ammonia molecules in the pores, whereas the strong acidity is primarily related to interactions between the NH_3 molecules and the zeolite pore walls. However, without any strong acid centers, the NH_3-TPD curves may still show a double peak feature if the pore is such a size that additional strain is put on the NH_3 hydrogen-bond network.

We also studied how the locations of the acid sites affect the adsorption of ammonia molecules. Placing the acidic sites at four different positions in MFI and including an equilibrated ammonia molecule, we calculated the radial distribution func-

tions (RDFs) for each pair of acid hydrogen atom plus ammonia nitrogen atom. The locations of the four acid sites in the primitive cell are shown in Figure 11, labeled as *a*, *b*, *c*, and *d*. Sites *a* and *b* are in the so-called zeta channel, and *c* and *d* are in the straight channel. According to the literature, *a* is the most stable acidic site.[13] GCMC simulations were performed at two temperatures, 300 and 450 K. Figure 12 displays the calculated RDFs for the acidic hydrogen and the ammonia nitrogen atom pairs at the different acid sites. At 300 K, the first peak, representing the probability of finding the first shell of ammonia molecules around the acid sites, is centered around 0.19 nm in the *a* curve, 0.23 nm in the *b* curve, and 0.21 nm in the *c* and *d* curves. Both the *c* and the *d* curves show an overlapped double-peak profile. At 450 K, the first peaks of all four curves change to about 0.2 nm, and the shoulders of the first peaks in the *c* and *d* curves disappear.

From these RDFs, we can deduce how ammonia molecules are adsorbed and desorbed. At 300 K, for the *a* and *b* sites in the zeta channel of MFI, only one molecule sits near the acidic site. In the straight channel *c* and *d* sites, on the other hand, two rows of ammonia molecules can be formed around the acid sites, as indicated by the two overlapped peaks. At 450 K, as the number of ammonia molecules is reduced, one row is left in the straight channel. The overlapped double peaks become one peak that shifts a little to the right in curves *c* and *d*.

The broad distribution of ammonia molecules around site *b* is due to two factors: (1) this site is in the middle of the zeta channel, which is difficult to access, and (2) the nearby, most stable site *a* is much easier to access. Because the RDF peak height reflects the probability of finding ammonia molecules at a given distance, the peak is broad when the probability is high for a wide range of positions. As the temperature increases, few ammonia molecules are left in the pores and the enthalpy contribution is more important than the entropy contribution. In this case, the *b* site is relatively more attractive to the molecules, so the first peak position of the *b* acid site moves from 0.24 to 0.20 nm.

4. Conclusion

Using force field parameters derived from high-level ab initio data, we used GCMC simulations to predict the NH_3-TPD curves in several common zeolites with different Si/Al ratios. By comparing the predictions with experimental data, we have demonstrated a new approach that can predict the relative NH_3-TPD curves for different zeolites. Such predictions are not feasible using existing empirical force fields.

The ability to predict NH_3-TPD curves from simulations based on first principles can enhance our understanding of the mechanism of zeolite acidities. Analysis of the molecular structures of the NH_3 molecules in zeolites at different temperatures reveals that the pore size is a critical factor that influences the curve features. The double peaks commonly referred to as weak and strong acids in the literature are controlled jointly by the size of the pore and the position and number of acidic centers. Although the weak acidity is primarily related to interactions among ammonia molecules in the pores and the strong acidity is primarily related to interactions between the NH_3 molecules and the zeolite pore walls, the NH_3-TPD curves may still show a double peak feature without any strong acid centers if the pore is such a size that additional strain is put on the NH_3 hydrogen-bond network.

Acknowledgment. Financial support from the National Science Foundation of China (Grant Nos. 20473052 and 10676021) and the National Basic Research Program of China (Grant Nos. 2003CB615804 and 2007CB209701) is gratefully acknowledged.

References and Notes

(1) Kramer, G.; van Santen, R.; Emeis, C.; Nowak, A. *Nature* **1993**, *363*, 529–531.
(2) Farneth, W.; Gorte, R. *Chem. Rev.* **1995**, *95*, 615.
(3) van Santen, R.; Kramer, G. *Chem. Rev.* **1995**, *95*, 637.
(4) Pinto, R.; Borges, P.; Lemos, M.; Lemos, F.; Védrine, J.; Derouane, E.; Ribeiro, F. *Appl. Catal., A* **2005**, *284*, 39.
(5) van Santen, R. *Catal. Today* **1997**, *38*, 377.
(6) Qi, X.; Kong, D.; Yuan, X.; Xu, Z.; Wang, Y.; Zheng, J.; Xie, Z. *J. Mater. Sci.* **2008**, *43*, 5626.
(7) Dondur, V.; Rakić, V.; Damjanović, L.; Auroux, A. *J. Serb. Chem. Soc.* **2005**, *70*, 457.
(8) Karge, H.; Dondur, V.; Weitkamp, J. *J. Phys. Chem.* **1991**, *95*, 283.
(9) Babitz, S.; Williams, B.; Miller, J.; Snurr, R.; Haag, W.; Kung, H. *Appl. Catal., A* **1999**, *179*, 71.
(10) Kassab, E.; Fouquet, J.; Allavena, M.; Evleth, E. *J. Phys. Chem.* **1993**, *97*, 9034.
(11) Teunissen, E. H.; Jansen, A. P. J.; van Santen, R. A.; Orlando, R.; Dovesi, R. *J. Chem. Phys.* **1994**, *101*, 5865.
(12) Bolis, V.; Busco, C.; Bordiga, S.; Ugliengo, P.; Lamberti, C.; Zecchina, A. *Appl. Surf. Sci.* **2002**, *196*, 56.
(13) Braendle, M.; Sauer, J. *J. Am. Chem. Soc.* **1998**, *120*, 1556.
(14) Eichler, U.; Braendle, M.; Sauer, J. *J. Phys. Chem. B* **1997**, *101*, 10035.
(15) Krossner, M.; Sauer, J. *J. Phys. Chem.* **1996**, *100*, 6199.
(16) Haase, F.; Sauer, J. *J. Am. Chem. Soc.* **1995**, *117*, 3780.
(17) Henninger, S.; Schmidt, F.; Nunez, T.; Henning, H. *Adsorption* **2005**, *11*, 361.
(18) Teraishi, K.; Akanuma, K. *Microporous Mater.* **1997**, *11*, 185.
(19) Jaramillo, E.; Chandross, M. *J. Phys. Chem. B* **2004**, *108*, 20155.
(20) Mabilia, M.; Pearlstein, R.; Hopfinger, A. *J. Am. Chem. Soc.* **1987**, *109*, 7960.
(21) Nicholas, J.; Hopfinger, A.; Trouw, F.; Iton, L. *J. Am. Chem. Soc.* **1991**, *113*, 4792.
(22) Schroeder, K.; Sauer, J. *J. Phys. Chem.* **1996**, *100*, 11043.
(23) de Vos Burchart, E.; Verheij, V.; van Bekkum, H.; van de Graaf, B. *Zeolites* **1992**, *12*, 183.
(24) Mayo, S.; Olafson, B.; Goddard, W., III *J. Phys. Chem.* **1990**, *94*, 8897.
(25) Boys, S. F.; Bemardi, F. *Mol. Phys.* **1970**, *19*, 553.
(26) Ahlrichs, R.; Bär, M.; Häser, M.; Horn, H.; Kölmel, C. *Chem. Phys. Lett.* **1989**, *162*, 165.
(27) Rizzo, R.; Jorgensen, W. *J. Am. Chem. Soc.* **1999**, *121*, 4827.
(28) Soto, J.; Myers, A. *Mol. Phys.* **1981**, *42*, 971.
(29) Snurr, R.; Bell, A.; Theodorou, D. *J. Phys. Chem.* **1993**, *97*, 13742.
(30) Karavias, F.; Myers, A. *Langmuir* **1991**, *7*, 3118.
(31) Widom, B. *J. Chem. Phys.* **1963**, *39*, 2808.
(32) Martin, M.; Siepmann, J. *J. Phys. Chem. B* **1999**, *103*, 4508.
(33) Lindahl, E.; Hess, B.; van der Spoel, D. *J. Mol. Model.* **2001**, *7*, 306.
(34) Feng, P.; Bu, X.; Pine, D. *Nature* **1997**, *389*, 368.
(35) Koningsveld, H.; Bekkum, H. *Acta Crystallogr., Sect. B* **1987**, *43*, 127.
(36) Passaglia, E. *Contrib. Mineral. Petrol.* **1975**, *50*, 65.
(37) Parrillo, D.; Gorte, R.; Farneth, W. *J. Am. Chem. Soc.* **1993**, *115*, 12441.
(38) Parrillo, D.; Gorte, R. *J. Phys. Chem.* **1993**, *97*, 8786.
(39) Chen, D.; Zhang, L.; Yi, C.; Dumesic, J. *J. Catal.* **1994**, *146*, 257.
(40) Garrone, E.; Onida, B.; Gabelica, Z.; Derouane, E. In *Zeolite Science 1994: Recent Progress and Discussions. Supplementary Materials to the 10th International Zeolite Conference, Garmisch-Partenkirchen, Germany, July 17−22, 1994*; Karge, H. G., Weitkamp, J., Eds.; Elsevier:Amsterdam, The Netherlands, 1995.
(41) Kramer, G.; Farragher, N.; van Beest, B.; van Santen, R. *Phys. Rev. B* **1991**, *43*, 5068.
(42) Berendsen, H.; Grigera, J.; Straatsma, T. *J. Phys. Chem.* **1987**, *91*, 6269.
(43) Katada, N.; Igi, H.; Kim, J.; Niwa, M. *J. Phys. Chem. B* **1997**, *101*, 5969.

JP811413M